

# Effect of nanosized graphite on properties of Sn–Bi solder

Li Yang · Chengchao Du · Jun Dai ·  
Ning Zhang · Yanfeng Jing

Received: 31 May 2013 / Accepted: 29 June 2013 / Published online: 17 July 2013  
© Springer Science+Business Media New York 2013

**Abstract** A novel Sn–Bi composite solder reinforced by nanosized graphite was studied. Effect of nanosized graphite content on spreadability was studied by spreading test. Microstructure of Sn–Bi solder and Sn–Bi composite solder was observed by scanning electron microscope. The tensile test and creep test for Sn–Bi solder and Sn–Bi composite solder joints were conducted in a micro-mechanical test system. The results show that the addition of nanosized graphite is harmful to the spreadability of Sn–Bi solder. The microstructure of Sn–Bi composite solder is refined gradually with the content of graphite increased. The ultimate tensile strength of Sn–Bi composite solders joints is reduced with the addition of nanosized graphite and the ultimate tensile strength of Sn–Bi + 0.07 wt% solder joint is almost unchanged compared with Sn–Bi solder joint. There is a great improvement in elongation of Sn–Bi + 0.07 wt% graphite solder joint. Furthermore, Sn–Bi + 0.07 wt% composite solder has a better creep performance compared with Sn–Bi solder.

## 1 Introduction

Sn–Pb solder was widely used as an interconnect material in electronics industry in the past. However, due to the consideration of environment protection, many kinds of substitutes for Sn–Pb solder were found, such as Sn–Cu, Sn–Ag, Sn–Zn, Sn–Ag–Cu (SAC) and Sn–Bi. Today, researchers are paying more and more attention on the reliability of solder joint. Composite solder is a common solder researchers employed to improve the reliability. Many kinds of reinforcing phases have been investigated.

Metallic particles, such as Ag, Ni and Cu, have been widely used in composite solder. Guo et al. [1] studied the effect of nanosized Ag particles on the comprehensive property of Sn–0.7Cu. They conducted wettability, mechanical performance, and creep-rupture life tests. The results show that the composite solder with 1 vol% Ag reinforcement addition exhibits the best comprehensive property as compared to the composite solders with other reinforcement volume fractions. Shi et al. [2] conducted the mechanical property of microsized Ag and Cu particle-reinforced Sn–0.7Cu solders. They observed that composite solders reinforced with microsized particles exhibit better creep strengthening than composite solders reinforced with nanosized particles, although the mechanical tensile shear strength of composite solder joints reinforced with nanosized particles may be higher than those reinforced with microsized particles. They also studied the constitutive relations for creep in Sn–0.7Cu composite solder reinforced with 5 vol% microsized Ag particles. They concluded that the activation energy of the Ag-particle-reinforced Sn–0.7Cu-based composite solder joint is higher than that of the Sn–0.7Cu solder joint. At the same time, the stress exponent of the Ag-particle-reinforced Sn–0.7Cu-based composite

---

L. Yang (✉) · J. Dai · Y. Jing  
School of Mechanical Engineering, Changshu Institute of  
Technology, No. 99, Hushan Street, Changshu 215500, Jiangsu  
Province, People's Republic of China  
e-mail: linlideyu@126.com

C. Du  
School of Materials Science and Engineering, Jiangsu University  
of Science and Technology, Zhenjiang 212000, Jiangsu  
Province, People's Republic of China

N. Zhang  
School of Mechanical and Electrical Engineering, Xuzhou  
Institute of Technology, Xuzhou 221008, Jiangsu Province,  
People's Republic of China

solder joint is higher than that of the Sn–0.7Cu solder joint [3].

Intermetallic compound particle is also a kind of reinforcement. Guo et al. [4] studied the creep and thermo-mechanical fatigue properties of in situ Cu<sub>6</sub>Sn<sub>5</sub> reinforced lead-free composite solder. They concluded that in situ Cu<sub>6</sub>Sn<sub>5</sub> reinforced composite solder has lower steady-state creep strain rate, higher stress exponent and higher shear stress. They also observed that in situ Cu<sub>6</sub>Sn<sub>5</sub> reinforcing particles could block the damages from propagation into the solder matrix.

There are also many papers about metallic oxide particles reinforced solders. These metallic oxide particles include TiO<sub>2</sub>, Al<sub>2</sub>O<sub>3</sub> and ZrO<sub>2</sub> et al. Tsao et al. [5] studied TiO<sub>2</sub> particles reinforced solder in details. They investigated the interfacial reaction, morphology of IMC, and shear strength in the Sn–3.5Ag–0.5Cu composite solder and BGA substrates during reflow. They stated that Sn–Ag–Cu composite solder reinforced with 1 wt% nanosized TiO<sub>2</sub> had a thinnest Cu<sub>6</sub>Sn<sub>5</sub> IMC layer at the solder/pad interface and a highest shear strength [5]. Tsao also studied the effect of nano-TiO<sub>2</sub> particles on the ultimate tensile strength (UTS) and yield strength (YS). He concluded that the addition of nano-TiO<sub>2</sub> particles promote a high nucleation density of second phase in the eutectic colony during solidification, reduce the average size of Ag<sub>3</sub>Sn size and contribute to a higher strength [6]. In another paper, Tsao et al. [7] studied effect of nano-TiO<sub>2</sub> particles on Sn–0.7Cu composite solder. The results show that the yield strength improvement was attributed to (1) the Hall–Petch effect due to β-Sn grain size refinement; (2) Orowan strengthening; (3) generation of geometrically necessary dislocations to accommodate CTE mismatch between the matrix and the second phase (Cu<sub>6</sub>Sn<sub>5</sub> and TiO<sub>2</sub>); and (4) load-bearing effects due to the presence of nano-sized reinforcements. Studies [8, 9] about composite solder reinforced with other metallic oxide particles showed similar results.

Some kinds of metal-unrelated materials were also applied in composite solder. Most of them, such as carbon nanotubes (CNTs), diamond particles, Si<sub>3</sub>N<sub>4</sub> particles, and SiC particles, have a high strength. Systematical investigations have been done by Nai and Han et al. about CNTs reinforced composite solder. They studied the effect of multiwalled CNTs (MWCNTs) on spreadability, melting point, density, mechanical properties, creep performance, electrical resistivity, and interfacial IMC growth. They concluded that MWCNTs could modify the spreadability, improve mechanical properties [10, 11], increase stress exponent and activation energy value [12], and suppress the growth of interfacial IMC [13]. Consider the combination between CNTs and matrix solders, Ni-coated CNTs were incorporated into Sn–3.5Ag–0.7Cu solder by Han et al. They investigated the effects of Ni-CNTs on the

physical, thermal and mechanical properties of SAC solder alloy. Decreased density and improved spreadability were found in SAC composite solder reinforced with Ni-CNTs. Mechanical characterization revealed an improvement in UTS and YS with addition of 0.05 wt% Ni-CNTs in SAC solder [14]. They also studied the improved creep performance of SAC/0.05 wt% Ni-coated CNTs by nanoindentation tests [15].

Although POSS (polyhedral oligomeric silsesquioxanes) particles are organic particles, they were incorporated into composite solder because of the special nano-structure. Guo et al. revealed the electromigration resistance of SnBi composite solder reinforced with POSS particles [16–18]. They also conducted hardness test of SAC composite solder and found that POSS particles increasing the hardness of SAC solder by means of refining Ag<sub>3</sub>Sn IMC particles.

In this paper, a novel Sn–Bi composite solder reinforced with nanosized graphite was fabricated. Effects of nanosized graphite on spreadability, microstructure, and mechanical properties were investigated. The creep performance of composite solder with 0.07 wt% nanosized graphite addition was studied.

## 2 Experiments

### 2.1 Materials

The composite solder pastes were fabricated by mechanical blending [19]. The matrix material used in this study was Sn–58Bi powder with an average diameter of about 43 μm. Graphite powder had an average size of 400 nm.

### 2.2 Spreadability and microstructure

About 0.25 g paste weighed from each prepared composite solder pastes was placed in the middle of each substrate, which was copper pads with dimension of 40 mm × 40 mm × 1 mm. These pads were all polished and cleaned with alcohol. The heating and cooling process of spreading samples is shown in Fig. 1.

Spreading coefficient which was used to weigh the spreadability of Sn–Bi solder and Sn–Bi composite solders was expressed as:

$$K = \frac{D - H}{D} \times 100\% \quad (1)$$

where  $K$  is spreading coefficient,  $D$  is the diameter of Sn–Bi ball which is equal to the Sn–Bi alloy spreading on the surface of copper substrate in mass, and  $H$  is the maximum height of solder alloy spreading on the surface of copper substrate.

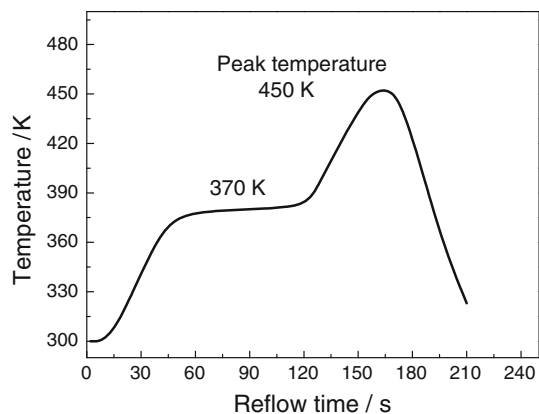


**Fig. 1** Reflow profile of Sn–Bi solder and its composite solder

The microstructure and fracture of Sn–Bi solder and its composite solders joints were observed by scanning electron microscope (SEM).

### 2.3 Miniature joint and tensile properties

The miniature joints (shown in Fig. 2) of Sn–Bi solder and Sn–Bi composite solders were prepared for tensile test. The heating and cooling process of miniature joints is shown in Fig. 1. The volume of solder alloy is 1 mm × 1 mm × 1 mm. A micro-mechanical test system (Micro-MTS, shown in Fig. 3) were designed and fabricated for tensile test and creep test. The UTS and elongation were recorded by Micro-MTS automatically.

### 2.4 Creep performance

Kanda and Kariya [20] evaluated creep properties of SAC by a multi-temperature stress relaxation test. We can conclude that lower stress relaxation rate means lower creep rate from Ref. [20]. So, the miniature joint was stretched and not stopped until the tensile stress up to about 20 MPa. Then the setup recorded the changing stress of miniature joint. The resistance to creep deformation could be distinguished from the relationship between time and stress clearly.

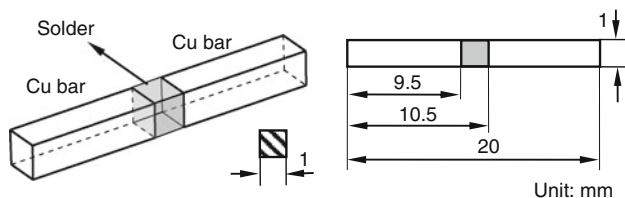


**Fig. 2** Geometry model of miniature joint

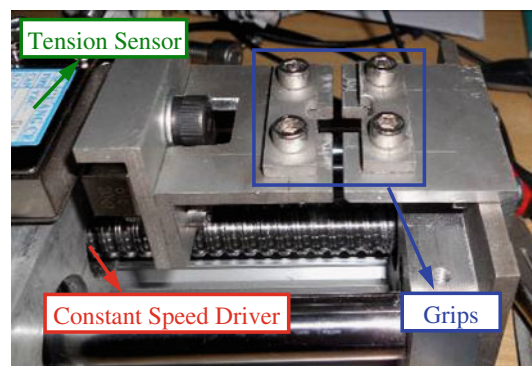


**Fig. 3** Part of micro-mechanical test system

## 3 Results and discussion

### 3.1 Effect of nanosized graphite content on spreadability of composite solder

Figure 4 shows the decreased spreading coefficient of composite solders with the addition of nanosized graphite. It indicates that addition of nanosized graphite can weaken the spreadability of Sn–Bi solder.

### 3.2 Effect of nanosized graphite content on microstructure of composite solder

Figure 5 reveals the microstructure of Sn–Bi solder and its composite solders. Figure 5a is the microstructure of Sn–Bi solder. Figure 5b, c, d, e show the microstructure of Sn–Bi composite solders. It can be seen from Fig. 5 that microstructure of Sn–Bi composite solders is refined gradually with the addition of nanosized graphite. The microstructure of composite solder with 0.07 wt% nanosized graphite addition has not changed greatly compared with that of Sn–Bi matrix solder. However, the composite solder with

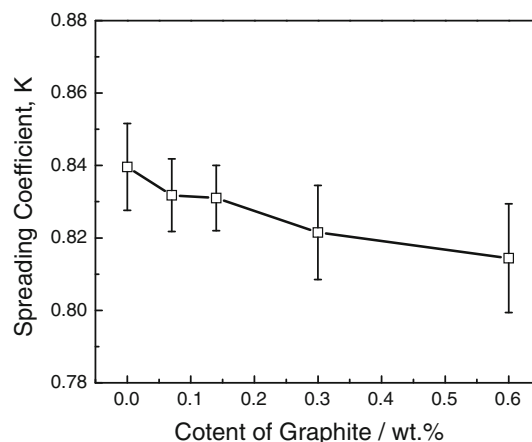


**Fig. 4** Effect of nanosized graphite on the spreadability of Sn–Bi composite solder

0.6 wt% nanosized graphite addition has the smallest microstructure. Nanosized graphite provides more centers for nucleation and leads to the refined microstructure.

### 3.3 Effects of nanosized graphite content on tensile properties of composite solder

Tensile test results revealed the influence of nanosized graphite on the UTS and elongation of Sn–Bi composite solder joint. The average UTS and elongation of joints are presented in Fig. 6. The average UTS of Sn–Bi joint is 57.84 MPa and is higher than that of its composite solder joints. The UTS of Sn–Bi + 0.07 wt% graphite composite solder is 57.57 MPa and has little of reduction compared with that of Sn–Bi matrix solder. The UTS of Sn–Bi + 0.14 wt%, Sn–Bi + 0.3 wt%, and Sn–Bi + 0.6 wt% composite solders joints is lower than that of Sn–Bi + 0.07 wt% composite solder joint. The elongations of Sn–Bi composite solder joints are all higher than that of Sn–Bi solder joint. However, the elongation of composite solder with 0.07 wt% nanosized graphite is the highest (about 2,019  $\mu\text{m}$ ).

According to 3.2 and Hall–Petch Relationship, smaller the microstructure is, higher the yield strength will be. However, high content of graphite separates the Sn–Bi matrix, and do damage to the strength by means of stress concentration.

Although smaller microstructure is observed in Sn–Bi + 0.14 wt%, Sn–Bi + 0.3 wt%, and Sn–Bi + 0.6 wt% composite solders, the UTS of their joints has not been improved. It is because of the damage effect that nanosized graphite leads to greater than the strengthen effect the refined microstructure causes.

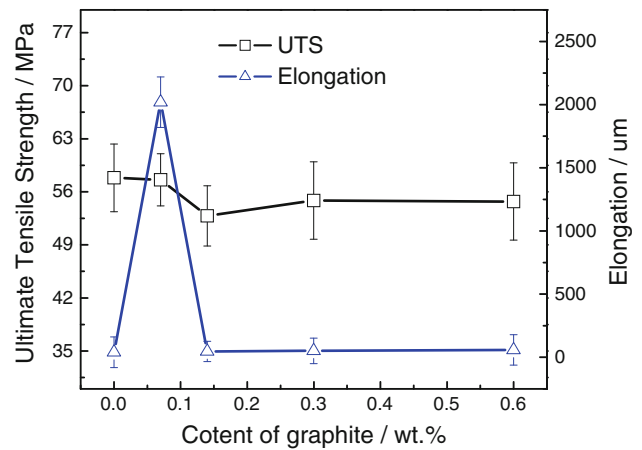


**Fig. 6** Effect of nanosized graphite on the UTS and Elongation of Sn–Bi solder and its composite solders joints

The microstructure of Sn–Bi + 0.07 wt% graphite composite solder is refined slightly and the content of nanosized graphite is very low. So the strengthen effect caused by refined microstructure is counterbalanced by the damage effect caused by nanosized graphite. This leads to the hardly changed UTS of Sn–Bi + 0.07 wt% graphite composite solder joint compared with that of Sn–Bi solder joint.

Figure 7 shows the joints after tensile test, stress distribution of joint in ABAQUS and tensile fracture of Sn–Bi + 0.07 wt% graphite composite solder joint. Figure 7a, b, c, d, e are the joints of Sn–Bi solder and its composite solders. It can be seen that joints in (a), (c), (d) and (e) were broken near the interface between Sn–Bi + x wt% graphite solder and copper bar. Figure 7f shows the stress

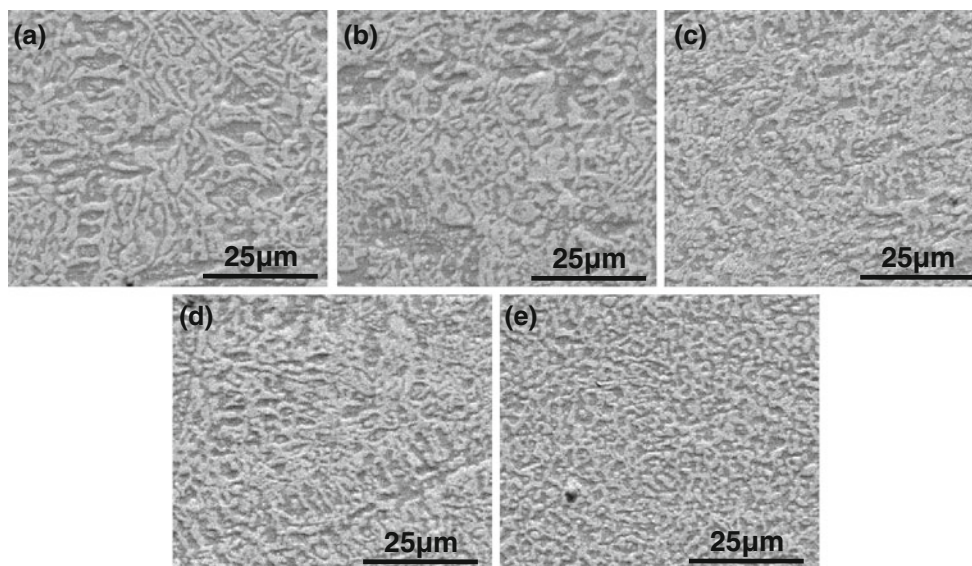


**Fig. 5** Microstructure of Sn–Bi solder and Sn–Bi composite solders **a** Sn–Bi, **b** Sn–Bi + 0.07 wt% Graphite, **c** Sn–Bi + 0.14 wt% Graphite, **d** Sn–Bi + 0.3 wt% Graphite **e** Sn–Bi + 0.6 wt% Graphite

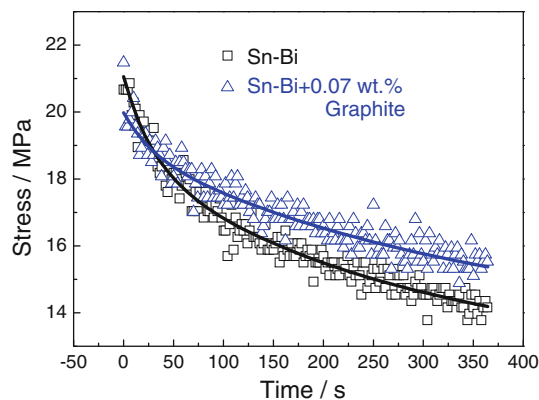


distribution of this kind of joints. The high stress areas that will become the failure area firstly are marked in it. This is the reason that these joints of Sn–Bi, Sn–Bi + 0.14 wt%, Sn–Bi + 0.3 wt%, and Sn–Bi + 0.6 wt% were broken near the interface between solder and copper bar. However, the Sn–Bi + 0.07 wt% graphite composite solder joint after tensile testing in Fig. 7b was fractured in the middle of solder joint. It is because of the improved ductility of Sn–Bi + 0.07 wt% graphite composite solder. The high stress in Fig. 7f can be relaxed rapidly by plastic deforming. The tensile fracture of Sn–Bi + 0.07 wt% graphite composite solder joint shown in Fig. 7g, h is tiny tough dimple which is typical characteristic of plastic fracture.

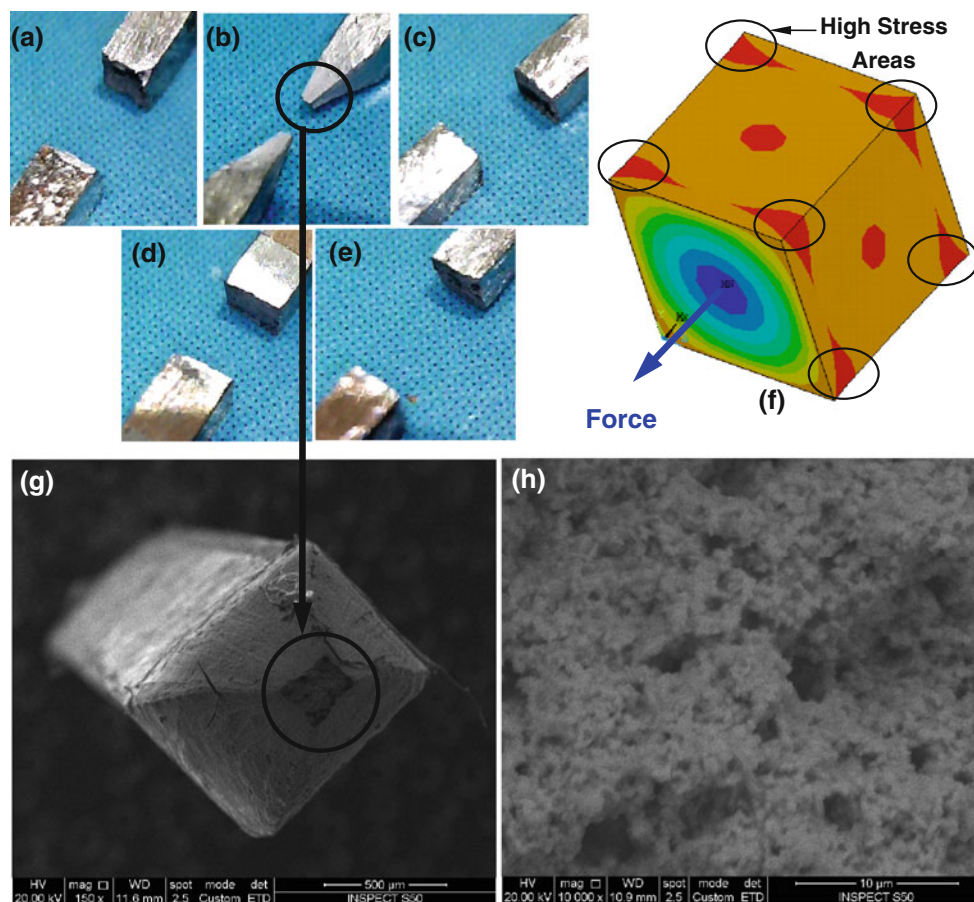
### 3.4 Creep performance of SnBi and SnBi/graphite

Figure 8 shows the changing stress of solder joints with the time prolonged during stress relaxation. The stress relaxation rate of Sn–Bi solder joint is larger than that of Sn–Bi + 0.07 wt% graphite composite solder joint. This means that Sn–Bi composite solder with 0.07 wt% graphite addition

has a lower creep rate compared with Sn–Bi solder under equal stress. Larger creep rate will be observed in the solder with smaller microstructure. However, the lower creep rate was observed in Sn–Bi + 0.07 wt% graphite composite solder which has a smaller microstructure. It is because of the



**Fig. 8** Stress relaxation curves of Sn–Bi and Sn–Bi + 0.07 wt% graphite composite solder



**Fig. 7** Joints after tensile test, stress distribution of joint in ABAQUS and tensile fracture of Sn–Bi + 0.07 wt% graphite composite solder joint. **a** Sn–Bi solder, **b** Sn–Bi + 0.07 wt% Graphite composite

solder, **c** Sn–Bi + 0.14 wt% Graphite composite solder, **d** Sn–Bi + 0.3 wt% Graphite composite solder, **e** Sn–Bi + 0.6 wt% Graphite composite solder

nanosized graphite that pinning the dislocations improves creep performance of Sn–Bi composite solder.

#### 4 Conclusions

In this work, spreadability, microstructure, ultimate tensile stress, elongation, and creep performance of Sn–Bi and its composite solder are investigated. Following conclusions can be made based on the results:

1. The addition of nanosized graphite is harm to the spreadability of Sn–Bi solder. The spreading coefficient is reduced from 0.84 to 0.81 with the increasing content of graphite from 0 to 0.6 wt%.
2. The microstructure of Sn–Bi and its composite solder is refined gradually with the content of graphite increased. This is because of the more centers for nucleation that nanosized graphite providing.
3. The ultimate tensile strength (UTS) of Sn–Bi solders joints is reduced with the addition of nanosized graphite and the UTS of Sn–Bi + 0.07 wt% is almost unchanged compared with Sn–Bi solder joint. There is a great improvement of elongation in 0.07 wt% graphite content.
4. The Sn–Bi + 0.07 wt% composite solder has a better creep performance compared with Sn–Bi solder. It is mainly because of pinning to dislocations caused by nanosized graphite.

#### References

1. F. Tai, F. Guo, Z.D. Xia et al., Processing and creep properties of Sn–Cu composite solders with small amounts of nanosized Ag reinforcement additions. *J. Electron. Mater.* **34**(11), 1357–1362 (2005)
2. Y.W. Shi, J.P. Liu, Y.F. Yan et al., Creep properties of composite solders reinforced with nano- and microsized particles. *J. Electron. Mater.* **37**(4), 507–514 (2008)
3. Y.W. Shi, Y.F. Yan, J.P. Liu et al., Constitutive relations for creep in a SnCu-based composite solder reinforced with Ag particles. *J. Electron. Mater.* **38**(9), 1866–1873 (2009)
4. F. Tai, F. Guo, M.T. Han et al., Creep and thermomechanical fatigue properties of in situ Cu<sub>6</sub>Sn<sub>5</sub> reinforced lead-free composite solder. *Mater. Sci. Eng., A* **527**, 3335–3342 (2010)
5. J.C. Leong, L.C. Tsao et al., Effect of nano-TiO<sub>2</sub> addition on the microstructure and bonding strengths of Sn<sub>3.5</sub>Ag<sub>0.5</sub>Cu composite solder BGA packages with immersion Sn surface finish. *J. Mater. Sci.: Mater. Electron.* **22**, 1443–1449 (2011)
6. L.C. Tsao, An investigation of microstructure and mechanical properties of novel Sn<sub>3.5</sub>Ag<sub>0.5</sub>Cu–xTiO<sub>2</sub> composite solders as functions of alloy composition and cooling rate. *Mater Sci Eng* **A529**, 41–48 (2011)
7. L.C. Tsao, C.H. Huang, C.H. Chung et al., Influence of TiO<sub>2</sub> nanoparticles addition on the microstructural and mechanical properties of Sn<sub>0.7</sub>Cu nano-composite solder. *Mater Sci Eng* **A545**, 194–200 (2012)
8. A.R. Geranmayeh, R. Mahmudi, M. Kangooie, High-temperature shear strength of lead-free Sn–Sb–Ag/Al<sub>2</sub>O<sub>3</sub> composite solder. *Mater Sci Eng* **A528**, 3967–3972 (2011)
9. Gain AK, Fouzder T, Chan YC et al. (2011) Microstructure, kinetic analysis and hardness of Sn–Ag–Cu–1 wt% nano-ZrO<sub>2</sub> composite solder on OSP–Cu pads. *Journal of Alloys and Compounds* 509(7):3319–3325
10. S.M.L. Nai, J. Wei, M. Gupta, Lead-free solder reinforced with multiwalled carbon nanotubes. *J. Electron. Mater.* **35**(7), 1518–1522 (2006)
11. S.M.L. Nai, J. Wei, M. Gupta, Effect of carbon nanotubes on the shear strength and electrical resistivity of a lead-free solder. *J. Electron. Mater.* **37**(4), 515–522 (2008)
12. S.M.L. Nai, J. Wei, M. Gupta, Using carbon nanotubes to enhance creep performance of lead free solder. *Mater. Sci. Technol.* **24**(4), 443–448 (2008)
13. S.M.L. Nai, J. Wei, M. Gupta, Interfacial intermetallic growth and shear strength of lead-free composite solder joints. *J. Alloy. Compd.* **473**, 100–106 (2009)
14. Y.D. Han, S.M.L. Nai, H.Y. Jing et al., Development of a Sn–Ag–Cu solder reinforced with Ni-coated carbon nanotubes. *J. Mater. Sci.: Mater. Electron.* **22**, 315–322 (2011)
15. Y.D. Han, H.Y. Jing, S.M.L. Nai et al., Creep mitigation in Sn–Ag–Cu composite solder with Ni-coated carbon nanotubes. *J. Mater. Sci.: Mater. Electron.* **23**, 1108–1115 (2012)
16. R.H. Zhang, G.C. Xu, X.T. Wang et al., Electromigration in Sn–Bi Modified with Polyhedral Oligomeric Silsesquioxane. *J. Electron. Mater.* **39**(12), 2513–2521 (2010)
17. J. Sun, G.C. Xu, Z.D. Xia et al., Effects of electromigration on resistance changes in eutectic SnBi solder joints. *J. Mater. Sci.* **46**, 3544–3549 (2011)
18. J. Sun, C.F. Peng, H.G. Yin et al., Influence of minor POSS molecules additions on the microstructure and hardness of Sn<sub>3</sub>Ag<sub>0.5</sub>Cu–xPOSS composite solders. *J. Mater. Sci.: Mater. Electron.* **23**, 1640–1646 (2012)
19. Li Yang, Effects of Ag particles content on properties of Sn<sub>0.7</sub>Cu solder. *J. Mater. Sci.: Mater. Electron.* **24**, 1405–1409 (2013)
20. Yoshihiko Kanda, Yoshiharu Kariya, Evaluation of creep properties for Sn–Ag–Cu micro solder joint by multi-temperature stress relaxation test. *Microelectronic Reliability* **52**, 1435–1440 (2012)